IBRO Reports 9 (2020) 302–309

Contents lists available at ScienceDirect

IBRO Reports

journal homepage: www.journals.elsevier.com/ibro-reports

Research Paper

Cerebrospinal fluid oxygen optimisation for rescue of metabolically challenged in vitro cortical brain tissue

Logan J. Voss [a,*], Nicola Whittle [a], Oliver Lamber [b], Gustav Envall [b], Jamie Sleigh [c]

[a] Anaesthesia Department, Waikato District Health Board, Hamilton, New Zealand
[b] School of Science and Engineering, University of Waikato, Hamilton, New Zealand
[c] Department of Anesthesia, Waikato Clinical Campus, University of Auckland, Hamilton, New Zealand

ARTICLE INFO

Keywords:
Hypoxia
Oxygen
Nanobubbles
Mouse
Cortex

ABSTRACT

Hypoxic-ischaemic brain injury is a major cause of morbidity and mortality internationally. Using an in vitro isolated cortex model, this study investigated the optimal cerebrospinal fluid oxygenation parameters for rescuing metabolically challenged cortical tissue. In particular, we asked whether maximizing oxygen content with oxygen nanobubbles could support improved tissue recovery. Mouse cortical slices were metabolically starved, followed by recovery in artificial cerebrospinal fluid (aCSF) containing different levels of dissolved oxygen ranging from mean(SD) 2(0.5) to 39(1.0) mg/L; with and without oxygen nanobubbles. Tissue recovery was assessed by quantifying and comparing the amplitude, length, high frequency content and event frequency of seizure-like events generated in no-magnesium aCSF at the beginning and end of the protocol. In general, there was improved recovery with increasing oxygen content up to 25–34 mg/L. The outcome of slices recovered in nanobubbled aCSF was no different to conventionally oxygenated slices with similar dissolved oxygen content. Dissolved oxygen content above 34 mg/L afforded no additional benefit. In conclusion, aCSF dissolved oxygen content of approximately 30 mg/L is optimal for cortical tissue recovery from metabolic starvation, which is easily achievable using conventional oxygenation methods. Oxygen in the form of nanobubbles does not appear to be readily available for tissue oxidative processes in this model.

Introduction

Brain hypoxia and ischaemia (stroke) is a leading cause of disability and death world-wide. Current acute treatments for stroke centre around restoring the blood supply to the affected area as quickly as possible. While controversial because of the potential for oxygen toxicity (Roffe et al., 2014), there is also considerable interest in the role of oxygen therapy for treatment of hypoxic-ischaemic conditions (Chan et al., 2014). One proposed avenue for delivering extravascular oxygen and glucose to the brain is via the circulating cerebrospinal fluid (CSF). While this principle has shown promise for spinal cord infarcts (Kanda et al., 2016), it remains largely untested for the brain. Provision of oxygenation via the CSF has been investigated using fluorocarbons as an oxygen carrier. This was successful in animal models (Osterholm et al., 1983) and a small human trial showed technical feasibility, however the fluorocarbons were found to diffuse through the brain parenchyma (Bell et al., 2006).

It is unclear what level of CSF oxygenation is appropriate for optimal recovery of brain function—or whether there may be detrimental effects associated with direct oxygen toxicity and/or "reperfusion" injury. A novel and increasingly popular approach for maximising oxygen content in solution is to supplement dissolved gas with oxygen nanobubbles (Matsuki et al., 2014). In theory it is possible to supersaturate the solution with nanobubbles because they have a very high internal pressure, thereby increasing gas solubility (Matsuki et al., 2014). Because of their negative charge, nanobubbles resist merging and are said to be very stable in solution for prolonged periods (Ebina et al., 2013; Matsuki et al., 2014). While a promising area of research, there are many issues surrounding nanobubbling bulk solutions for tissue oxygenation, not least of all identifying and measuring the level of gas content in nanobubble form (Leroy and Norisuye, 2016; Kim et al., 2018). Also, given their stability, it is not clear whether the oxygen in nanobubbles is available for tissue metabolism.

These ideas are challenging to test in vivo, requiring invasive and technically difficult experiments. We therefore sought to investigate the effect of artificial CSF (aCSF) oxygenation on cerebrocortical recovery

* Corresponding author at: Anaesthesia Department, Waikato District Health Board, Pembroke St, Hamilton, New Zealand.
E-mail address: logan.voss@waikatodhb.health.nz (L.J. Voss).

https://doi.org/10.1016/j.ibror.2020.10.007
Received 28 June 2020; Accepted 30 October 2020
Available online 4 November 2020

from hypoxia-ischaemia in an in vitro model. We used mouse cortical slices because an avascularised preparation is ideal for modelling an in vivo brain infarct – where the tissue relies on diffusion of oxygen and glucose from the bathing aCSF. The intensity of the ischemic-hypoxic metabolic stress was instantiated by perfusion with a hypoxic and hypoglycemic solution. The aims of this study were twofold: to optimise oxygen content in aCSF for tissue recovery following metabolic starvation; and to compare aCSF oxygenation using conventional methods with nanobubble oxygenation.

Experimental procedures

Ethics statement

The methods for anesthetising and euthanasing the mice were approved by the Waikato Animal Ethics Committee and comply with the standards provided in Standard Operating Procedure Number: 9.

Solution preparation

Solution composition

Three different solutions were used to perfuse the slices. "Normal" artificial cerebrospinal fluid (aCSF) was prepared in distilled water with a composition similar to physiological cerebrospinal fluid, with NaCl (130 mM), KCl (2.5 mM), $MgCl_2$ (1.0 mM), $CaCl_2$ (2.0 mM), $NaHCO_3$ (2.5 mM), Glucose (20 mM), Hepes (10 mM) and NaOH (3.5 mM). "No-Mg" aCSF was as above, except that $MgCl_2$ was replaced by an additional 2.5 mM of KCl. The metabolic starvation ("M-S") solution was the same as no-Mg aCSF, but with glucose (20 mM) replaced by mannitol (20 mM), which has similar oncotic qualities, but reduced metabolic potential for the cells. To achieve a low oxygen concentration of approximately 2 mg/L (approximately 35 mmHg in lab settings) in the M-S aCSF, distilled water was boiled for 4−5 min, kept in an enclosed container without air and allowed to cool down to room temperature, before adding the aCSF salts.

Solution oxygenation

Oxygenation of the normal aCSF and no-Mg aCSF solutions was done by bubbling oxygen (95 %, Perfecto2, Invacare, Auckland, NZ) for approximately 15 min prior to, and continuously during contact with slice tissue. We have termed this "conventional oxygenation". Nanobubbled oxygenation was achieved by infusing oxygen nanobubbles into solution using a cavitation method (Dynaflow Inc., Maryland, USA). The ability of this device to generate oxygen nanobubbles in bulk solution was tested by adding aCSF salts to nanobubbled distilled water and premade aCSF. Increasing the salt concentration destabilises invisible nanobubbles (Nirmalkar et al., 2018), causing them to coalesce into visible microbubbles. Dense microbubble formation was clearly and consistently observed when salts were added to the nanobubbled solutions (n = 5) (Fig. 1), but never with conventionally oxygenated solutions (n = 4). The microbubbles formed gradually rose to the surface and dissipated over a period of 1−2 min.

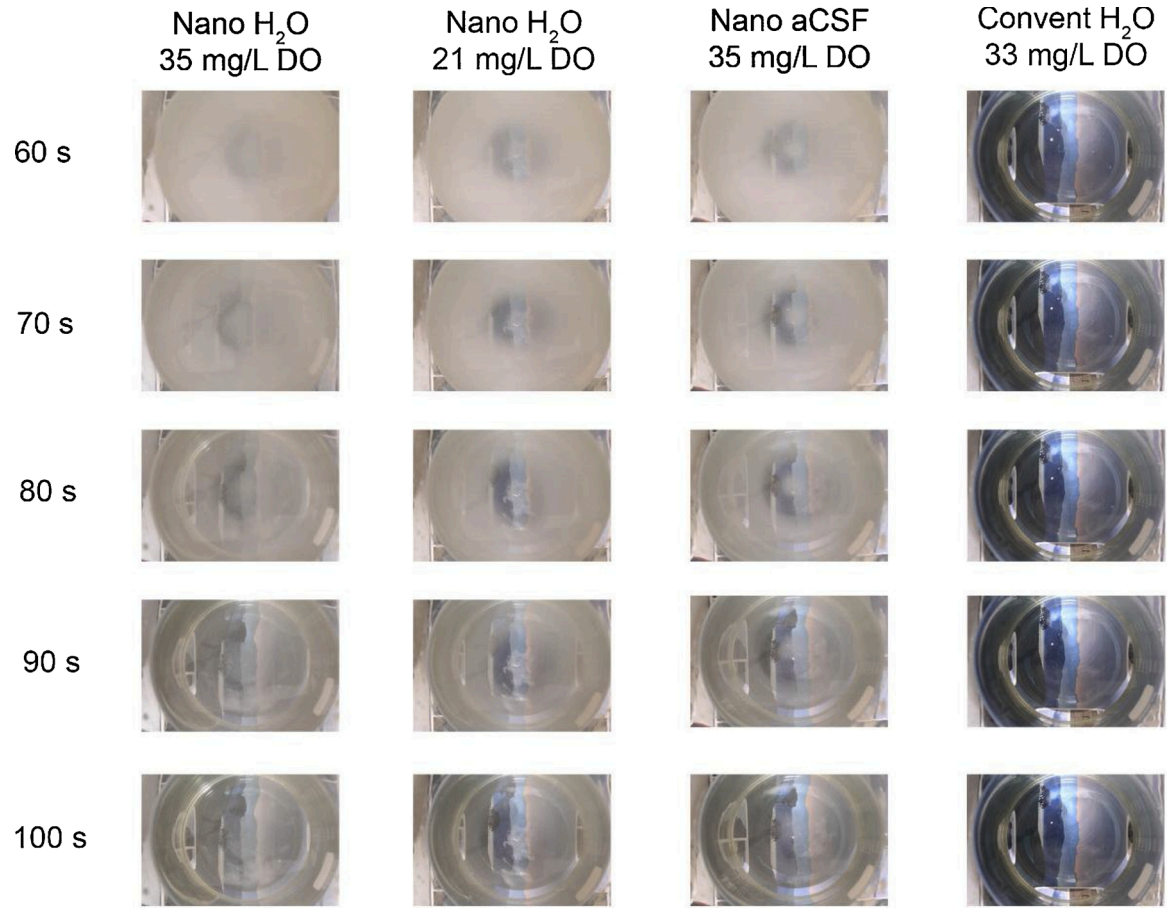

Fig. 1. Microbubble generation in four oxygenated solutions, 60–100 s after adding artificial cerebrospinal fluid (aCSF) salts. The first two columns show nanobubbled (Nano) distilled water with differing levels of dissolved oxygen (DO) (achieved by altering the oxygen inflow while nanobubbling). The third column shows nanobubbled aCSF and the fourth conventionally oxygenated distilled water. The photographs were taken looking vertically down on the beaker. A high contrast picture was placed under the beaker to help visualize the changes in bubble density. Microbubble generation is obvious in all three nanobubbled solutions, irrespective of dissolved oxygen level or prior salt content. Conventionally oxygenated water showed no microbubble formation.

Oxygen content measuring

Before perfusing any solution, dissolved oxygen concentration was measured (Optical probe, Orion Versa Star Pro, ThermoFisher Scientific, Auckland NZ), giving mg/L dissolved oxygen content. It was important to know what the oxygen levels were in the slice perfusion bath, where the tissue was exposed to the aCSF. However, the bath oxygen content could not be measured directly while perfusing slices because of the size of the optical probe. Therefore, in a pilot investigation without tissue slices, dissolved oxygen content (maximised with conventional bubbling) in the slice perfusion bath was measured directly at different temperatures — and compared to the levels recorded in the reservoir solution feeding the bath. At room temperature, 15 °C and 10 °C (at an aCSF flow rate of 15 mL/min), there was an oxygen loss at the bath of 1.5 %, 9.0 % and 15.0 %, respectively. Using these correction factors, the oxygen content of the slice bath was approximated from the measured pre-perfused oxygen level. Oxygenation levels presented in the results are bath-corrected values.

Tissue preparation and recording

Brain tissue was extracted from male or female mice of the strain C57. One mouse was sacrificed for each experimental day and two slices were used for experiments that day. The mice were anesthetised with CO_2, decapitated and the brain extracted in a standardised fashion. The extracted brain was swiftly submerged in ice-cold normal aCSF and sliced coronally into 400 µm thick sections using a vibrotome (Campden Instruments Ltd, Sileby, Leics, UK). Three scalpel cuts were made through the entire depth of the cortex and subcortical white matter; one in the midline (through the corpus callosum) and one in each hemisphere midway between the midline and the lateral border of the slice (see Fig. 2). This was done in to provide four independent cortical regions for recording and analysis. Subsequently, the slices were immersed in no-Mg aCSF at room temperature (approximately 21 °C) for at least 60 min. Exposure to no-Mg aCSF activates the tissue by unblocking NMDA receptors (Aram and Lodge, 1988), resulting in the generation of repeating, spontaneous paroxysmal events commonly known as seizure-like events (SLEs). SLE activity is sensitive to hypoxic challenge (Voss et al., 2020) and provides a relatively non-invasive electrophysiological method for quantifying tissue viability over time (Voss et al., 2013).

Data recording

The slices were transferred one at a time to a submersion-style perfusion bath (Kerr Scientific Instruments, Dunedin, NZ) which was continuously flowed with the aCSF solution of choice, at an adjustable flow rate. Initially, no-Mg SLE activity was recorded using four 75 µm Ag/AgCl electrodes inserted into the cortex, one within each quarter section (labelled e1-e4 in Fig. 2). A disc Ag/AgCl electrode positioned distant to the slice in the recording bath was used as a common reference/ground. The electrodes were positioned extracellularly to monitor field potential. The analog signal was amplified (Model 3000 differential amplifier, A-M Systems, USA) and converted to a digital signal (PowerLab, ADInstruments, Australia) that was analysed later. The analog signal was filtered with: high pass - 1 Hz, low pass - 300 Hz and a notch filter at 50 Hz. The gain was x1000 and the sampling rate 1000/s.

Experimental procedures

Metabolic starvation

A summary of the metabolic starvation (simulated "hypoxia-ischaemia") experimental protocol is illustrated in Fig. 3. Initially, room temperature no-Mg aCSF was perfused at a rate of 5−10 ml/min in order to produce stable baseline SLE activity. The no-Mg aCSF was oxygenated by conventional bubbling to a level of approximately 25 mg/L oxygen concentration. Electrode placement was adjusted in order to record SLE activity that was independent at each location. Activity in at least three out of four electrodes was required to proceed with the experiment, otherwise a new slice was introduced. When stable SLE activity was established, a 20-minute metabolic starvation period (2 mg/L oxygen) was started by perfusing the M-S aCSF at a flow rate of 15 mL/min. This resulted in the rapid termination of all SLE activity (see Fig. 3). Thereafter, normal aCSF "recovery" solution was perfused for 30 min at a flow rate of 15 mL/min. The temperature (10−21 °C), oxygen content (2−39 mg/L) and oxygenation method (conventional and nanobubbled) of this recovery solution was manipulated according to the goals of the investigation and was the basis for differentiating the experimental groups. Finally, no-Mg aCSF (at the same flow rate as baseline) was reintroduced for at least 40 min to determine slice outcome. As at baseline, the no-Mg aCSF was oxygenated by conventional bubbling to a level of approximately 25 mg/L. The SLE activity that had reemerged by the end of the recording was compared with baseline activity.

Nanobubble supplementation of dissolved oxygen levels

At reduced aCSF flow rates, dissolved oxygen becomes the limiting factor for maintaining population activity in slices (Ivanov and Zilberter, 2011). To test whether oxygen in nanobubble form could provide a reservoir for supplementing dissolved oxygen levels, two protocols were investigated. Firstly, the rate of reduction in dissolved oxygen content in

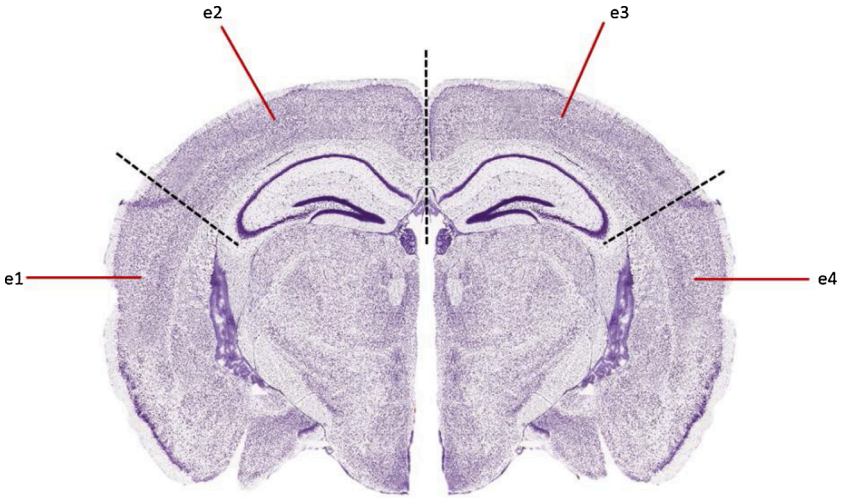

Fig. 2. Coronal rodent slice showing the recording electrode arrangement, e1-e4. The dashed black lines show the approximate location of the scalpel cuts made to isolate the sections of cortical tissue. Modified from (Paxinos and Watson, 1998).

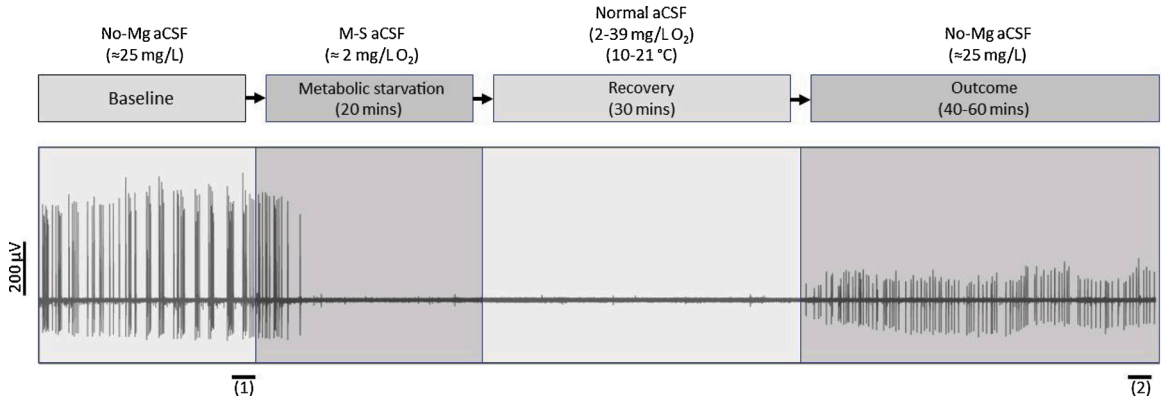

Fig. 3. Schematic representation of the experimental protocol (top), with an example recording showing the seizure-like event (SLE) activity time-course (bottom). Each of the fine vertical lines in the recording are a single SLE. Labelled segments (1) and (2) represent the position of the two analysis periods for comparing outcome to baseline SLE characteristics. In this case the recovery period aCSF was oxygenated to 38 mg/L at 15°C.

conventionally oxygenated and nanobubbled aCSF (in standing, open beakers without slices) was compared over a 40-minute period (n = 9 each). The hypothesis was that the dissolved oxygen content in the nanobubbled solution should decline more slowly. Secondly, slices generating no-Mg SLE activity were perfused at three stepwise reductions in aCSF flow rate (10, 5, 2.5, 0 mL/min), with one group exposed to conventionally oxygenated aCSF and a second group to nanobubbled aCSF (n = 15 each). The hypothesis was that SLE activity would remain stronger at the lower flow rates in the nanobubbled aCSF.

Data analysis

Each electrode produced a raw data signal in the form of a continuous time-line of electric potential. Customised scripts in Matlab (The Mathworks inc., Natick, MA, USA) were used to extract different parameters of the SLE activity, namely SLE length, amplitude, high frequency activity and event frequency. This paramatisation is illustrated in Fig. 4.

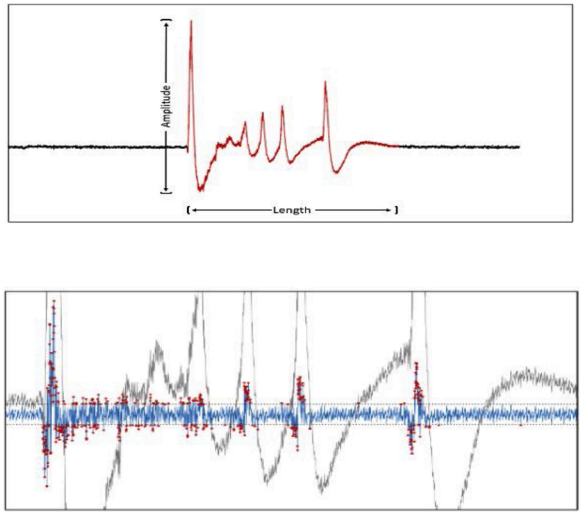

Fig. 4. Example of the paramatisation of a single seizure-like event (SLE). Length was manually determined as the time-course of each event (highlighted in red in the top figure); amplitude was the absolute value of the maximum peak-trough voltage deflection; Quantification of SLE high frequency activity is illustrated in the bottom figure. The recorded SLE (zoomed grey trace) was high-pass filtered below 20 Hz (blue trace). The noise threshold was determined (horizontal dotted black traces) and the absolute value of the voltage values above and below this threshold (red dots) were summed to give the "size" of the high frequency component of the event.

Metabolic starvation

From all recordings, two segments containing at least four SLEs each were exported: one segment from the baseline period just before initiation of the metabolic insult; and one from the end of the recording, following slice recovery (labelled (1) and (2) in Fig. 3). The beginning and the end of the event was manually identified and SLE parameters (detailed below) averaged across the four events. SLE length was determined as the time extent of the event (expressed in seconds); SLE amplitude was the difference between the highest and the lowest recorded voltage in the event, expressed as microvolts; SLE high frequency activity was a measure of the oscillatory activity above 20 Hz. This was quantified by first applying a 20 Hz high pass filter to the signal. A small segment of background "noise" was manually selected to create a filter based on the mean voltage +/− two standard deviations. The voltage of the recordings that lay outside of this filter were summed as the absolute value to give the "size of the high frequency component of the event. SLE frequency was calculated manually from the raw data signal, by determining how many SLE events appeared in a five-minute period, expressed as events per minute. The quantified variables thus obtained from the baseline and outcome segments were averaged and compared by calculating the percentage change from the baseline value, a negative value indicating that SLE activity had not recovered fully to the baseline level.

Nanobubble supplementation of dissolved oxygen levels

Using the same analysis methods as above, the effect of aCSF flow rate on SLE frequency, amplitude and length was compared between conventionally oxygenated and nanobubbled groups.

Statistical methods

Statistical analysis was carried out using GraphPad Instat (version 3.03). Data normality was assessed using the Kolmogorov-Smirnov test and the appropriate parametric or non-parametric test applied. Where three or more independent groups were compared, either a 1-way ANOVA or Kruskal-Wallis test was applied. When comparing 2 independent groups, either an unpaired *t*-test or Mann-Whitney test was applied. One-sample data were analysed with either the Wilcoxon rank sum test or 1-sample *t*-test. The Chi-squared test was used to determine the degree of significance between groups with binary dependent variables. Multiple regression analysis was used to investigate which factors were influential for outcome. Unless otherwise stated the data are expressed as mean(SD) in the text and mean(SEM) in the figures. A p-value <0.05 was considered statistically significant.

Results

aCSF oxygen content testing

Seven groups were exposed to differing levels and methods of aCSF oxygenation following the metabolic challenge. Dissolved oxygen levels ranged from mean(SD) 2(0.5) to 39(1.0) mg/L (Fig. 5b). The highest levels of dissolved oxygen (38(1) mg/L and 39(1) mg/L) were achieved by cooling the aCSF to 15 °C and 10 °C, respectively. These cooled aCSF oxygen levels were not statistically different, therefore the data for these two groups were pooled. Control experiments determined that aCSF cooling was unlikely to have significantly confounded these results (see supplementary data). All other groups were at room temperature (approximately 21 °C).

While the oxygen content in nanobubble form could not be quantified in absolute terms, the presence of nanobubbles was confirmed by observing the production of microbubbles following addition of salts to nanobubbled water, an effect known as "induced coalescence"(Kim et al., 2018). The microbubbles were highly likely to be oxygen because a small but significant reduction in oxygen content was observed following salt addition, compared to no change following addition of salts to conventionally oxygenated water (% change of −8(2) mg/L compared to 0.3(1.2) mg/L, $p = 0.0002$ and $p = 0.7$, respectively, 1-sample *t*-test). This result also suggests that the oxygen meter, utilizing an optical measurement method, could at least partially detect oxygen nanobubble content in bulk solution.

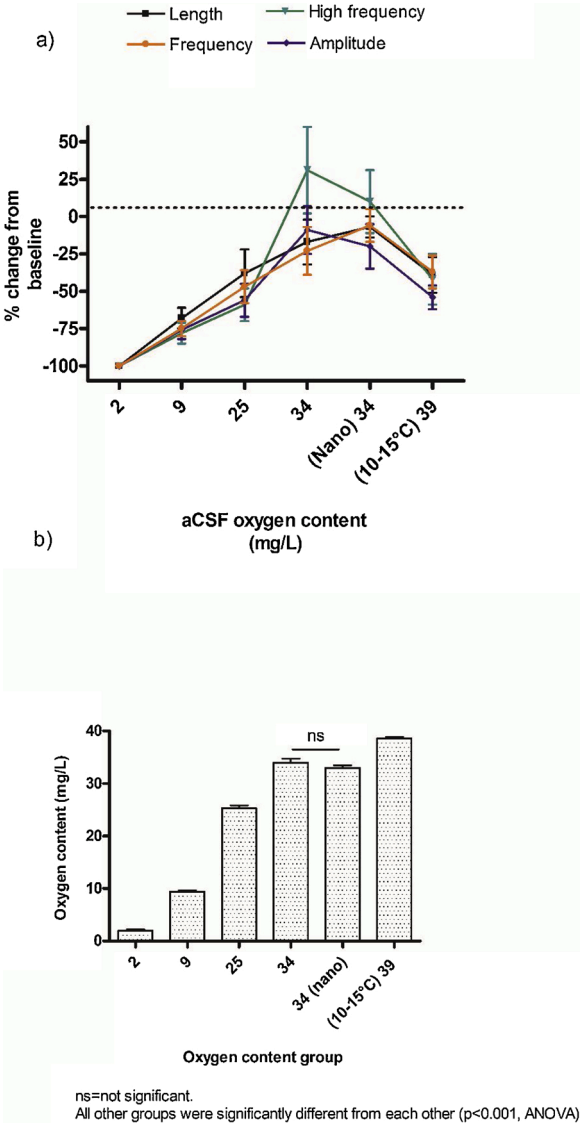

Fig. 5. Graphs showing a) SLE parameter restoration (% baseline) according to recovery in different oxygen levels and b) corresponding aCSF oxygen levels for each group. Nano refers to the nanobubbled group.

SLE recovery from metabolic starvation

Tissue recovery was quantified according to the four SLE parameters at each oxygen level and is shown graphically in Fig. 5a. Statistical significance for comparisons between oxygen levels for each parameter are given in the matrix tables (Table 1). In general, there was improved recovery with increasing oxygen content up to 25–34 mg/L. The only groups that fully recovered from the hypoxic stress were the 34 mg/L conventionally oxygenated and nanobubbled groups ($p > 0.05$ for all SLE parameters compared to baseline, 1-sampled *t*-test). The outcome of slices recovered in nanobubbled aCSF was no different to conventionally oxygenated slices with similar dissolved oxygen content. Dissolved oxygen content above 34 mg/L was detrimental for slice recovery, with all recovery parameters reduced compared to baseline ($p < 0.005$, Wilcoxon rank sum test).

Nanobubble supplementation of dissolved oxygen levels

We found no evidence that nanobubbles in aCSF could supplement dissolved oxygen content. In open, standing beakers of oxygenated aCSF, after 40 min dissolved oxygen levels had reduced by 8.5 %(mean change from 33.6–30.8 mg/L) in the nanobubbled group and by 7.7 % (mean change from 32.1–29.6 mg/L) in the conventionally bubbled group ($p = 0.46$, unpaired *t*-test). SLE frequency was significantly reduced at 0 mL/min compared to 10 mL/min in both conventionally oxygenated and nanobubbled groups; and at 2.5 ml/min in the conventionally oxygenated group (Fig. 6). There was no difference in SLE amplitude or high frequency activity between groups at any flow rate (unpaired t-tests). A small increase in SLE length was noted in the nanobubbled group at 2.5 ml/min ($p = 0.03$, Friedman test). These data suggest that oxygen in nanobubble form does not provide a source of dissolved oxygen.

Discussion

In this study we sought to optimise oxygen content in aCSF for tissue recovery following a metabolic challenge simulating a hypoxic-ischaemic insult. This was done by altering the dissolved oxygen content, with and without oxygen nanobubbles. In summary, the results show that a 20-minute perfusion of hypoxic-hypoglycemic solution caused a measurable, lasting deterioration in cortical slice viability, evident in all parameters. The degree of recovery was dependent upon aCSF oxygen content delivered during the post-insult period, with higher oxygen beneficial up to approximately 34 mg/L. For a given level of dissolved oxygen, the addition of oxygen nanobubbles did not supplement dissolved oxygen content, or tissue recovery. We can conclude that tissue recovery in the nanobubbled group was due to the dissolved oxygen, not oxygen nanobubbles.

A recovery ceiling of 34 mg/L oxygen could be explained by direct toxic effects at the higher oxygen levels. The pathogenesis of central nervous system oxygen toxicity is not well understood, but is thought to involve an excess of reactive oxygen species, resulting in oxidation of cellular components, metabolic dysregulation and in extreme cases, excitotoxicity and seizures (Manning, 2016; Wingelaar et al., 2017). Few studies have directly measured the brain oxygen levels that correlate with the onset of oxygen toxicity. Demchenko (Demchenko et al., 2005) identified a threshold pO_2 of 900 mmHg for seizures in rats breathing 5 atmospheres of oxygen, which equates to 40 mg/L at 37 °C. CNS seizures

Table 1
Matrix tables indicating significant differences in parameter outcome comparing each recovery oxygen level (white diagonal squares, Kruskal-Wallis test with Dunn's Multiple Comparisons Test). In the grey diagonal squares, arrows indicate a significant difference in baseline parameter ($p < 0.05$, Kruskal-Wallis test with Dunn's Multiple Comparisons Test). N refers to the nanobubble group. ns = non-significant.

a) SLE Length

	2 (n=20; 5 slices)	9 (n=42; 13 slices)	25 (n=44; 11 slices)	34 (n=20; 5 slices)	34 (N) (n=24; 6 slices)	39 (n=24; 6 slices)
2		ns	<0.01	<0.001	<0.001	<0.001
9			ns	ns	<0.01	ns
25				ns	ns	ns
34					ns	ns
34 (N)						ns
39 (10-15°)						

c) SLE High frequency

	2	9	25	34	34 (N)	39
2		ns	ns	<0.001	<0.001	ns
9			ns	<0.001	<0.05	ns
25				<0.05	ns	ns
34		↑	↑		ns	ns
34 (N)		↑	↑			ns
39 (10-15°)		↑	↑			

d) SLE Amplitude

	2	9	25	34	34 (N)	39
2		ns	<0.01	<0.001	<0.001	<0.001
9			ns	<0.01	<0.01	ns
25				ns	ns	ns
34					ns	ns
34 (N)						ns
39 (10-15°)		↓				

e) SLE Frequency

	2	9	25	34	34 (N)	39
2		ns	<0.01	<0.001	<0.001	<0.001
9			ns	ns	<0.01	ns
25		↓		ns	ns	ns
34		↓			ns	ns
34 (N)						ns
39 (10-15°)						

have been observed at lower inspired levels of between 2–3 atmospheres (Bitterman, 2004). Inspired oxygen at 3 atmospheres equates to a brain pO_2 of around 300 mmHg (Muir et al., 2016), which converts to 13 mg/L (at 37 degrees). Clearly, there is some variability and uncertainty around the toxic oxygen threshold for seizures. Because we used a seizure-like model to gauge tissue viability, oxygen toxicity in the form of seizure is difficult to identify. However, two observations are relevant and imply toxic oxygen effects at higher oxygen levels. Firstly, all parameters showed sub-optimal recovery at the highest dissolved oxygen level of 39 mg/L (Fig. 5), compared to full recovery in the 34 mg/L groups. Secondly, slices that were recovered in 34 mg/L oxygen and above exhibited a disproportionately high rate of SLE development during the high-oxygen recovery period in "normal" aCSF (results not shown). While not unheard of, it is unusual for SLE activity to develop in cortical slices perfused with normal aCSF (Smith et al., 1989). It should also be noted that seizures are an extreme manifestation of oxygen toxicity and presumably more subtle effects occur below this threshold.

The existence of nanobubbles in bulk solution was proposed as long ago as the 1960s (Alheshibri et al., 2016). While difficult to explain theoretically, empirical data now strongly supports their existence (Ohgaki et al., 2010; Nirmalkar et al., 2018). Measuring nanobubbles in solution is not straight forward and a number of techniques have been proposed. High-tech methods such as dynamic light scattering and scanning electron microscopy (Ohgaki et al., 2010) do not differentiate between gases and solids, raising the very important issue of particulate contamination (Leroy and Norisuye, 2016). Ultrasound may be a more specific method (Leroy and Norisuye, 2016), but this has not been routinely used or validated for this purpose. Similarly, blood gas analysis is not validated for quantifying nanobubble content, although it has been used previously within this context (Matsuki et al., 2014). Simple visual qualitative methods, such as green laser scattering and "induced coalescence" have also been proposed (Kim et al., 2018). While appealing in its simplicity, laser scattering is also susceptible to particulate contamination. The principle of induced coalescence is the visualization of microbubble "clouds" from the coalescence of otherwise invisible nanobubbles (Kim et al., 2018) In theory, this could be achieved by any intervention that disrupted nanobubble stability. Salts are known to destabilise nanobubbles (Nirmalkar et al., 2018) and in this study nanobubbled distilled water and aCSF turned opaque with microbubbles immediately following addition of aCSF salts. While we were not able to quantify nanobubble size or density in this study, we concluded from these observations that nanobubbles had been successfully generated. It is noteworthy that the relationship between measured dissolved oxygen and nanobubble content is complex and dependent on nanobubble size (Kim et al., 2018). For this reason, the dissolved oxygen levels in the nanobubbled group are not straight forward to interpret and probably reflect a combination of dissolved and nanobubble oxygen content.

That no difference in outcome was observed in the nanobubble group supports a number of possible interpretations: 1) toxic effects may have limited any potential benefit of elevated oxygen content in the form of nanobubbles or; 2) the total oxygen content between the nanobubbled and conventionally oxygenated solutions may not have been sufficiently different or; 3) because of their stability, the oxygen in nanobubble form may not have been readily available to the tissue. The latter raises an interesting point of discussion. The benefit of nanobubble-infused oxygen in CSF may not lie in attaining supersaturated levels per se, but in providing a long-lasting oxygen reservoir capable of maintaining dissolved oxygen levels higher for longer. This would be especially pertinent if applied to circulating CSF in vivo, where the flow rates would need to be extremely low. To test this, we investigated the effect of reduced aCSF flow rates on SLE activity (thus, significantly limiting tissue oxygen supply (Ivanov and Zilberter, 2011)), comparing conventionally oxygenated and nanobubbled aCSF. As expected, a degradation in SLE activity (that is, a reduction in SLE frequency) was observed at the lower flow rates, however there was no significant difference between oxygenation groups. We also observed that dissolved oxygen content in aCSF samples reduced at a similar rate in conventionally oxygenated and nanobubbled solutions. Thus, oxygen nanobubbles do not appear to supplement dissolved oxygen levels.

A previous investigation in a rabbit spinal cord ischaemia model, found that CSF perfusion of oxygen nanobubbles improved neurological recovery compared to non-oxygenated CSF (Kanda et al., 2016). Unfortunately, this study did not include a comparison group with CSF oxygenated by conventional dissolution. On the basis of our findings, it's very likely the recovery benefit they found was achieved through dissolved oxygen in the nanobubbled group. Certainly, the nanobubble technology we employed in this study always generated a concomitant high level of dissolved oxygen in the aCSF.

For decades, slice electrophysiologists have regarded the amplitude of extracellularly recorded population activity to be the best criterion for judging slice viability (Fountain et al., 1988), with some justification (Voss et al., 2013). It is interesting to note from this study that all SLE parameters were affected by the hypoxic insult. Within the context of hypoxic-ischaemic damage therefore, it seems that a reduction in SLE length and frequency are also strongly indicative of deteriorating tissue viability. Comparing the baseline characteristics across groups identified some subtle differences, particularly lower SLE amplitude and frequency in the 9 mg/L group. This was unlikely to reflect poor tissue

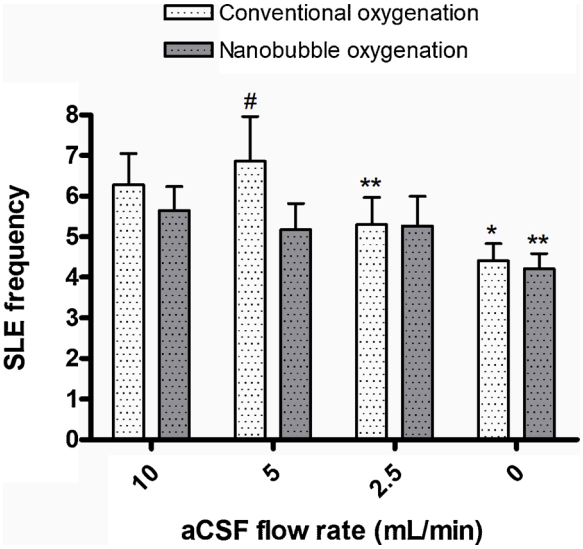

Fig. 6. Effect of aCSF flow rate on seizure-like event (SLE) frequency in conventional oxygenation and nanobubble oxygenation groups.
*$p < 0.05$, compared to 10 mL/min (Friedman test, Dunn's multiple comparisons test).
**$p < 0.01$, compared to 10 mL/min (Friedman test, Dunn's multiple comparisons test).
#$p < 0.05$, compared to 2.5 and 0 mL/min (Friedman test, Dunn's multiple comparisons test).

viability in this group, because high frequency activity was elevated — and we would expect all parameters to be reduced in poorly viable tissue (Voss et al., 2020). There is no obvious explanation for this difference. However, the consistent trend in the pattern of recovery across the groups (see Fig. 5) suggests these baseline differences are unlikely to have affected the overall findings of the investigation.

A potential criticism of this investigation is that slice oxygenation requirements and metabolism are different to the in vivo situation, therefore conclusions drawn form a study such as this are difficult to extrapolate to the in vivo setting. Firstly, the slices were studied at room temperature and the temperature during hypoxia exposure is a determinant of tissue recovery (see supplementary information). Consequently, the tissue recovery in this study may have exceeded that possible at 37° in vivo. Secondly, slice oxygen requirements for maintaining neuronal activity is high compared to in vivo, in the region of 300–400 mmHg, compared to <100 mmHg (Ivanov and Zilberter, 2011). It should be noted however, that the hypoxic brain in vivo effectively becomes an island of avascularised tissue sitting in CSF, very similar to the slice model (but without the physical disconnection). In this situation, it is likely that in vivo ischaemic tissue will behave more like an in vitro slice in terms of its oxygen response. Several additional questions remain outstanding from this study. Firstly, the cortical slices utilized in this study were just 400 μm thick, compared to a cortical thickness in the human brain of several mm. The results of this study do not inform regarding tissue recovery characteristics at deeper levels. Secondly and as already discussed, quantification of oxygen nanobubbles is fraught with difficulties. While we confirmed the presence of nanobubbles, we have no data on the density of bubbles achieved. The lack of nanobubble effect in this study needs to be seen with this limitation in mind.

In summary, aCSF dissolved oxygen content of approximately 30 mg/L is optimal for cortical tissue recovery from metabolic challenge. This level of oxygenation is easily achievable using conventional macrobubbling methods. Nanobubble oxygenation does not further improve tissue recovery and may not be a useful technology for rescue of the brain tissue via CSF.

Conflicts of interest

None.

Funding

This research did not receive any specific grant from funding agencies in the public, commercial, or not-for-profit sectors.

CRediT authorship contribution statement

Logan J. Voss: Investigation, Conceptualization, Writing - original draft, Writing - review & editing. **Nicola Whittle:** Conceptualization, Methodology. **Oliver Lamber:** Investigation, Formal analysis. **Gustav Envall:** Investigation, Formal analysis. **Jamie Sleigh:** Conceptualization, Writing - review & editing.

Appendix A. Supplementary data

Supplementary material related to this article can be found, in the online version, at doi:https://doi.org/10.1016/j.ibror.2020.10.007.

References

Alheshibri, M., Qian, J., Jehannin, M., Craig, V.S.J., 2016. A history of nanobubbles. Langmuir 32, 11086–11100.
Aram, J.A., Lodge, D., 1988. Validation of a neocortical slice preparation for the study of epileptiform activity. J. Neurosci. Methods 23, 211–224.
Bell, R.D., Powers, B.L., Brock, D., Provencio, J.J., Flanders, A., Benetiz, R., Strause, J., Frazer, G., Kramer, M.S., Hesson, D., Barnitz, J., Osterholm, J.L., 2006. Ventriculolumbar perfusion in acute ischemic stroke. Neurocrit. Care 5, 21–29.
Bitterman, N., 2004. CNS oxygen toxicity. Undersea Hyperb. Med. 31, 63–72.
Chan, Y.F.Y., Katz, M., Moskowitz, A., Levine, S.R., Richardson, L.D., Tuhrim, S., Chason, K., Barsan-Silverman, K., Singhal, A., 2014. Supplemental oxygen delivery to suspected stroke patients in pre hospital and emergency department settings. Med. Gas Res. 4, 1–7.
Demchenko, I.T., Luchakov, Y.I., Moskvin, A.N., Gutsaeva, D.R., Allen, B.W., Thalmann, E.D., Piantadosi, C.A., 2005. Cerebral blood flow and brain oxygenation in rats breathing oxygen under pressure. J. Cereb. Blood Flow Metab. 25, 1288–1300.
Ebina, K., Shi, K., Hirao, M., Hashimoto, J., Kawato, Y., Kaneshiro, S., Morimoto, T., Koizumi, K., Yoshikawa, H., 2013. Oxygen and air nanobubble water solution promote the growth of plants, fishes, and mice. PLoS One 8, 1–8.
Fountain, S.B., Hennes, S.K., Teyley, T.J., 1988. Aspartame exposure and in vitro hippocampal slice excitability and plasticity. Fundam. Appl. Toxicol. 11, 221–228.
Ivanov, A., Zilberter, Y., 2011. Critical state of energy metabolism in brain slices: the principal role of oxygen delivery and energy substrates in shaping neuronal activity. Front. Neuroenerg. 3, 1–13.
Kanda, K., Adachi, O., Kawatsu, S., Sakatsume, K., Kumagai, K., Kawamoto, S., Saiki, Y., 2016. Oxygenation of the cerebrospinal fluid with artificial cerebrospinal fluid can ameliorate a spinal cord ischemic injury in a rabbit model. J. Thorac. Cardiovasc. Surg. 152, 1401–1409. https://doi.org/10.1016/j.jtcvs.2016.04.095. Available at:
Kim, S., Kim, H., Han, M., Kim, T., 2018. Generation of sub-micron (nano) bubbles and characterization of their fundamental properties. Environ. Eng. Res. 24, 382–388.
Leroy, V., Norisuye, T., 2016. Investigating the existence of bulk nanobubbles with ultrasound. Chemphyschem 17, 2787–2790.
Manning, E.P., 2016. Central nervous system oxygen toxicity and hyperbaric oxygen seizures. Aerosp. Med. Hum. Perform. 87, 477–486.
Matsuki, N., Ishikawa, T., Ichiba, S., Shiba, N., Ujike, Y., Yamaguchi, T., 2014. Oxygen supersaturated fluid using fine micro/nanobubbles. Int. J. Nanomed. 9, 4495–4505.
Muir, E.R., Cardenas, D.P., Duong, T.Q., 2016. MRI of brain tissue oxygen tension under hyperbaric conditions. Neuroimage 133, 498–503.
Nirmalkar, N., Pacek, A.W., Barigou, M., 2018. On the existence and stability of bulk nanobubbles. Langmuir 34, 10964–10973.
Ohgaki, K., Quoc, N., Joden, Y., Tsuji, A., Nakagawa, T., 2010. Physicochemical approach to nanobubble solutions. Chem. Eng. Sci. 65, 1296–1300.
Osterholm, J.L., Alderman, J.B., Triolo, A.J., D'Amore, B.R., Williams, H.D., Frazer, G., 1983. Severe cerebral ischemia treatment by ventriculosubarachnoid perfusion with an oxygenated fluorocarbon emulsion. Neurosurgery 13, 381–387.
Paxinos, G., Watson, C., 1998. The Rat Brain in Stereotaxic Coordinates, 4th edition. Academic press, London.
Roffe, C., Nevatte, T., Crome, P., Gray, R., Sim, J., Pountain, S., Handy, L., Handy, P., 2014. The Stroke Oxygen Study (SO2S) - a multi-center, study to assess whether

routine oxygen treatment in the first 72 hours after a stroke improves long-term outcome: study protocol for a randomized controlled trial. Trials 15, 1–11. Available at: Trials.
Smith, D.A.S., Connick, J.H., Stone, T.W., 1989. Effect of changing extracellular levels of magnesium on spontaneous activity and glutamate release in the mouse neocortical slice. Br. J. Pharmacol. 97, 475–482.
Voss, L.J., van Kan, C., Sleigh, J.W., 2013. Quantitative investigation into methods for evaluating neocortical slice viability. BMC Neurosci. 14, 137.
Voss, L.J., Van, Kan C., Envall, G., Lamber, O., 2020. Impact of variation in tissue preparation methodology on the functional outcome of neocortical mouse brain slices. Brain Res. 1747, 147043 https://doi.org/10.1016/j.brainres.2020.147043. Available at:
Wingelaar, T.T., van Ooij, P.-J.A.M., van Hulst, R.A., 2017. Oxygen toxicity and special operations forces diving: hidden and dangerous. Front. Psychol. 8, 1263.